

12. START-UP AND OPERATIONS

Robert A. Krakowski Tak-Kuen Mau Mohammad Z. Hasan
Kenneth R. Schultz Giorgio L. Varsamis Clement P. C. Wong

Contents

12.1.	INTRODUCTION	12-1
12.2.	PLASMA START-UP	12-2
12.2.1.	Features of Start-Up Code	12-3
12.2.2.	Results of Simulations	12-11
12.2.3.	Summary and Critical Issues	12-25
12.3.	PLANT START-UP	12-26
12.3.1.	Start-Up Requirements	12-26
12.3.2.	Partial- and Over-Power Operations	12-28
12.4.	SUMMARY AND CONCLUSIONS	12-31
	REFERENCES	12-32

12. START-UP AND OPERATIONS

12.1. INTRODUCTION

The time required for plasma start-up and shut-down for the steady-state ARIES-I design is short when compared with the burn period, and is considered to be an occasional event in the reactor lifetime. The start-up, therefore, can be performed slowly and under optimal conditions (*e.g.*, minimum power, stress, *etc.*). Furthermore, a rapid current ramp-up is undesirable because of increased power requirements and the demands on the poloidal-field (PF) coil system to keep the plasma in equilibrium. For the ARIES-I study, a quantitative modeling and assessment of the plasma start-up scenario was carried out, assuming disruption-free plasma and ensuring compatibility of the auxiliary-power system needed for start-up with the current-drive system required for steady-state operation. While a minimum-power requirement or minimum-energy input has been used frequently as a criterion in designing the start-up phase, it is of secondary importance in the context of a steady-state reactor.

Considerations of the various reactor subsystems, such as first wall, blanket, divertor, and power conversion also impose constraints on the plant start-up and partial- and over-power operations. These constraints are mainly due to the temperature and thermal stress limits of the materials used in the subsystems, and to the power requirements for magnet cool-down, blanket heat-up, and coolant circulation.

In this section, both the plasma and engineering aspects of the start-up procedure for ARIES-I are examined in detail. In particular, Sec. 12.2 describes a plasma start-up code that is used to simulate the current ramp-up and plasma ignition scenarios for a tokamak reactor. The coupling of the fusion plasma with the PF-coil system and the reactor first wall can also be modeled. Preliminary simulation results indicate that a reasonable start-up scenario with an ~ 2400 s duration using auxiliary heating by the current-drive system is indeed possible. Section 12.3 contains an assessment of the engineering constraints on the plant start-up and its various modes of power operations. No major critical issue has been uncovered by this study. In Sec. 12.4, conclusions and recommendations for future work are given.

12.2. PLASMA START-UP

In this section, various plasma-physics aspects of the start-up and operation of a tokamak reactor are examined in the context of the ARIES-I design. A typical reactor plasma start-up procedure consists of the following sequence of events: plasma initiation, current initiation, current and density ramp-up, auxiliary heating to ignition, and approach to steady-state operating conditions. Specifically, plasma initiation, current start-up, and current ramp-up have been demonstrated in a notable experiment on PLT [1] using only lower-hybrid waves. A one-hour-long tokamak discharge sustained entirely by lower-hybrid waves has recently been reported in TRIAM-1M [2], and a record current-drive efficiency, $\gamma (\equiv n_e I_\phi R_T / P_{CD})$, of 0.34×10^{20} A/W-m² was obtained on JT-60 [3]. The data base for lower-hybrid start-up and current drive, therefore, is strong and the physics understanding is mature.

Generally, a number of plasma start-up scenarios can be envisaged [4]. In ARIES-I, a low-density current ramp-up scenario based on lower-hybrid current drive is proposed, with a limit on the power input of not more than 20 MW. Electronic phasing of the lower-hybrid waveguide grille is a crucial element in this approach. At 0° phasing and modest power levels, the plasma is initiated at full radius. The increased power input is balanced against plasma convective losses through toroidal drift that can be adjusted by the vertical field [5]. By introducing a non-zero phase shift between adjacent waveguides in the grille, the current can be initiated and ramped up. Once the full current is reached, a programmed fueling and auxiliary-heating schedule can be activated to bring the plasma to full fusion-power production. Transition to fast-wave current drive (FWCD) should be timed to provide adequate current ramp-up assist and auxiliary heating to the plasma. Throughout the start-up phase, constraints related to plasma-current ramp rates (≤ 1 MA/s for disruption mitigation), electron runaway, poloidal-field ramp-up rates (≤ 1 T/s), and thermomechanical responses of the fusion power core are applied.

Only a limited number of start-up scenarios, going from current ramp-up to steady state, were considered and the results should be regarded as preliminary and non-exhaustive. Section 12.2.1 describes the tokamak-specific features of the start-up simulation code used in the study. Section 12.2.2 gives preliminary results of a start-up scenario leading to the ARIES-I reference steady-state parameters. The thermomechanical response of the first wall for this reference scenario is also presented. Section 12.2.3 contains a summary of the simulation results and lists a number of critical issues.

12.2.1. Features of Start-Up Code

Estimates of the ARIES-I current and fusion-power ramp-up parameters have been made using a time-dependent, profile-averaged (zero-dimensional) plasma-circuit simulation code. This code solves a set of particle and power-balance equations for the plasma. These equations are coupled in turn to a set of circuit equations that describe the magnetic interactions between the plasma and the various coil systems. The code utilizes a multi-species plasma model that includes electrons, fuel ions, impurities, and fusion ash. A Fokker-Planck formalism is used to describe both charged-particle fusion-product slowing down and electron-ion energy equi-partition. Assuming density and temperature profiles of the form $[1 - (r/a)^2]^{\alpha_n, \alpha_T}$ and on-axis and edge-plasma safety factors, respectively q_o and q_a , the equilibrium current-density and magnetic-field profiles are approximated. In addition to the basic plasma and field-coil responses (*e.g.*, currents, voltages, densities, temperatures, powers), the code also estimates the first-wall thermal and mechanical responses. The start-up code, originally developed for the reversed-field-pinch (RFP) reactor, is described in detail in Refs. [6] and [7]; only modifications made to model for the tokamak are given in this section. All quantities in this section are in MKS units except for temperature in keV, power in MW, and current in MA.

12.2.1.1. Plasma model

In this start-up code, the plasma is modeled as a torus with a circularized cross section of minor radius r_p . For an elongated plasma of half-height b and equatorial plane half-width a (elongation $\kappa = b/a$), triangularity δ , and major radius R_T , the equivalent plasma radius is [8]

$$r_p = a \kappa \left(1 - \frac{0.233 \delta}{A} \right) \left[\frac{2 J_1(\delta)}{\delta} \right]^{1/2}. \quad (12.2-1)$$

An equivalent first-wall radius is taken as $r_w = r_p/x$ ($x \leq 1$) when computing the thermomechanical response in Sec. 12.3.

A cylindrical one-dimensional (1-D) MHD equilibrium solver is used to compute the field and current profiles from a given pressure profile. With $\mu \equiv \mu_o \mathbf{j} \cdot \mathbf{B}/B^2$ and p denoting the plasma pressure, the following equilibrium equations are solved:

$$-\frac{\partial B_\phi}{\partial r} = \mu_o j_\theta = \mu B_\theta + \mu_o \frac{\partial p}{\partial r} \cdot \frac{B_\phi}{B^2}, \quad (12.2-2)$$

$$\frac{1}{r} \frac{\partial}{\partial r} (r B_\theta) = \mu_o j_\phi = \mu B_\phi - \mu_o \frac{\partial p}{\partial r} \cdot \frac{B_\theta}{B^2}. \quad (12.2-3)$$

For the RFP case, $\mu(r)$ is specified to satisfy experimental observation $\mu(r) \propto 1 - (r/a)^8$. For the case of a tokamak, $\mu(r) = \mu_o j_\phi(r)/B_\phi$ is used with $j_\phi(r)$ being approximated by $[1 - (r/r_p)^2]^{\alpha_J}$ and $\alpha_J = (q_o/q_a)^{-1}$. While this 1-D approximation is adequate for the high-aspect-ratio circular RFP, applicability to the ARIES-I configuration is less certain. The impact of the approximate profiles on the start-up results, however, should be small since the equilibrium current-density and magnetic-field profiles are only used to calculate the plasma inductance for use in the circuit analysis (Sec. 12.2.1.3) and the plasma ohmic dissipation (corrected for neoclassical trapped-electron effects [9]). This neoclassical correction is applied to the classical parallel-field electrical resistivity, $\eta_{||}^{CL}$, in a tokamak of inverse aspect ratio, $\epsilon \equiv 1/A \equiv a/R_T$, resulting in $\eta_{||}^{NEO}$ given by [9]

$$\frac{\eta_{||}^{CL}}{\eta_{||}^{NEO}} = \left[1 - \frac{f_T(\epsilon)}{1 + \zeta \nu_{*e}} \right] \left[1 - \frac{C_R f_T(\epsilon)}{1 + \zeta \nu_{*e}} \right], \quad (12.2-4)$$

where ν_{*e} is the electron collisionality and

$$\begin{aligned} f_T(\epsilon) &= 1 - \frac{(1 - \epsilon)^2}{(1 - \epsilon^2)^{1/2}(1 + 1.46 \epsilon^{1/2})}, \\ C_R &= \frac{0.56}{Z_{eff}} \frac{3 - Z_{eff}}{3 + Z_{eff}}, \\ \nu_{*e} &= \frac{r_p (B_\phi/B_\theta)}{\epsilon^{3/2} (T_e/m_e)^{1/2}} \nu_{ei}, \\ \nu_{ei} &= 9.1 \times 10^{17} n_e \ln \Lambda T_e^{-3/2}, \\ \zeta &= 0.58 + 0.20 Z_{eff}. \end{aligned} \quad (12.2-5)$$

The plasma-energy confinement time, τ_E , is modeled by the inverse-quadrature relation between neo-Alcator and Goldston confinement times, respectively τ_{NA} and τ_G [12]:

$$\tau_E = \left[\tau_{NA}^{-2} + (H_G \tau_G)^{-2} \right]^{-1/2}, \quad (12.2-6)$$

where

$$\begin{aligned} \tau_{NA} &= 1.92 \times 10^{21} n_i a R_T^2, \\ \tau_G &= 3.7 \times 10^{-5} \kappa^{0.5} \left(\frac{A_i}{1.5} \right)^{0.5} I_\phi P_H^{-0.5} R_T^{-1.75} a^{-0.39}, \end{aligned} \quad (12.2-7)$$

and A_i is the atomic mass number of the fuel ions and P_H is total heating power. The Goldston confinement multiplier, H_G , in Eq. (12.2-6) is fixed at 1.5. For purposes of establishing a fueling algorithm, the ion-particle confinement time, τ_p , is taken to be $4\tau_E$.

Synchrotron-radiation power loss, P_{CYC} , is calculated using the locally applied global model described in Sec. 2.2, and is found to scale as

$$P_{CYC} \propto (1 - \mathfrak{R})^{1/2} n_e^{1/2} T_e^{5/2} B_\phi^{5/2}, \quad (12.2-8)$$

where \mathfrak{R} is the first-wall reflectivity. In ARIES-I, the silicon-carbide first wall is quite lossy ($\mathfrak{R} \simeq 0.4$), and both T_e and B_ϕ are high. Thus, P_{CYC} is comparable to the transport power loss and far exceeds bremsstrahlung radiation losses. Line radiation losses from carbon, oxygen, and iron impurities, and Z_{eff} are estimated with a coronal equilibrium model [13].

Two models [10, 11] are used to estimate the pressure-gradient-driven bootstrap current, I_{BS} . Defining the Shafranov beta as $\beta_{IO} \equiv 2\mu_o p_o / B_\theta^2$, where $B_\theta = \mu_o I_\phi / (2\pi a S)$, $S = [(1 + \kappa^2)/2]^{1/2}$, and p_o is the peak pressure, the bootstrap-current fraction, f_{BS} , is given by

$$f_{BS} \equiv \frac{I_{BS}}{I} \phi = f_1 \left[C_1 - C_2 \left(\frac{\alpha_T}{\alpha_p} \right) - C_3 \left(\frac{\alpha_T}{\alpha_p} \right) \frac{n_e T_i}{Z_{eff} p_o} \right] \frac{\beta_{IO}}{A^{1/2}}, \quad (12.2-9)$$

for the model used in Ref. [10]. In this expression $\alpha_p = \alpha_n + \alpha_T$, $C_1 = 2.1$, $C_2 = 1.3$, $C_3 = 1.2$, and $f_1 = 0.24$. For the approach recommended in Ref. [11],

$$f_{BS} = \frac{\beta_\theta (1 + \alpha_p) (\alpha_n C_n + \alpha_T C_T)}{2\delta^{1/2}} \int_0^1 \frac{x^{7/2} (1 - x^2)^{\alpha_p - 1}}{1 - (1 - x^2)^{\alpha_J + 1}} dx, \quad (12.2-10)$$

where β_θ is the poloidal beta, $C_n = 1.5 + 3.1/Z_{eff}^{1.26}$, and $C_T = 1.3 - 0.93/Z_{eff}^{0.83}$. Typically, f_{BS} is small for the initial start-up conditions assumed and increases as the plasma beta is raised. In the simulations, f_{BS} is assumed to increase to the ARIES-I design-point value and, once achieved, is fixed at that value. In order to account for the pedestal density profile, which is used in the ARIES systems code but not included in the burn code, f_{BS} is multiplied by a factor of 1.5 with the constraint that $f_{BS} \leq 0.68$, which is the steady-state value used in the systems code.

12.2.1.2. Current ramp-up model

The current ramp-up model described in Ref. [14] is used to relate the radio-frequency (RF) current-drive power, P_{CD} , needed to drive the non-inductive part of the current transient, I_{RF} . With the plasma loop voltage given by $V_\phi = P_\Omega / I_\phi$ in terms of the ohmic power dissipation, P_Ω , and $E_{||} \equiv V_\phi / (2\pi R_T)$,

$$\frac{P_{CD}}{I_{RF}} = \frac{1 - \Gamma_o E_{||}}{\Gamma_1}, \quad (12.2-11)$$

where, for lower-hybrid waves [14],

$$\Gamma_o = \Gamma_{LH} = \frac{9.848 \times 10^{21} (1/N_{Z2}^2 - 1/N_{Z1}^2)}{n_e(Z_{eff} + 2) \ln \Lambda \ln(N_{Z1}/N_{Z2})}, \quad (12.2-12)$$

$$\Gamma_1 = \frac{\Gamma_o}{2\pi R_T K}, \quad (12.2-13)$$

K is a constant (~ 0.39), and Γ_1 can be interpreted as the current-drive efficiency in the absence of $E_{||}$. The assumed square-wave spectrum of parallel refractive indices over which RF electron interactions occur is defined by $N_{Z1} = 2.0$ and $N_{Z2} = 1.5$. These values for the refractive indices are chosen to give a normalized current-drive efficiency, γ , to the steady-state value from the systems code, and to ensure penetration of the wave to the plasma core.

We will show below [Eq. (12.2-22)] that the self- and mutual inductance of coils and plasma can be combined into an equivalent inductance, L_E . Then, the RF current driven during start-up is determined by the following simple circuit equation,

$$I_{RF} = I_\phi + \frac{L_E}{R_p} \frac{dI_\phi}{dt}, \quad (12.2-14)$$

where R_p is the evolving plasma resistance, $R_p \simeq 2R_T \eta_{||}^{NEO}/r_p^2$. A correction for the bootstrap current is implied in Eq. (12.2-14). The heating power delivered to the plasma is given by

$$P_H = P_{RF} - L_E I_\phi \dot{I}_\phi, \quad (12.2-15)$$

of which $\sim 99\%$ is assumed to be deposited in the electrons. Note that the term $L_E I_\phi \dot{I}_\phi$ in Eq. (12.2-15) represents the power that goes into the poloidal-field energy in the plasma.

For low-density lower-hybrid current start-up, it is necessary to monitor the condition for electron runaway (*i.e.*, when electron dynamical friction falls below the $eE_{||}$ accelerating force). The runaway condition is $E_{||}/E_D \geq 0.01$, where the Dreicer field, E_D , is given by

$$E_D \simeq 10^{-3} \left(\frac{e}{\epsilon_o}\right)^2 \ln \Lambda \frac{n_e}{T_e}. \quad (12.2-16)$$

Once the plasma current reaches the steady-state level, it is assumed that FWCD takes over as the density and fusion power are simultaneously ramped to the steady-state condition. Then, an empirical expression for the fast-wave efficiency, γ_{FW} , is used for this part of the simulation and is given by

$$\gamma_{FW} = 0.72 \langle T_e \rangle^{0.77} (0.014 + 0.235\beta_\phi), \quad (12.2-17)$$

where $\langle T_e \rangle$ is the volume-averaged electron temperature.

12.2.1.3. Plasma circuit model

A wide range of plasma start-up scenarios can be envisaged. These scenarios require programming the current-drive power, the fueling rate, and the PF-coil voltages. To ensure a smooth approach of the plasma to the design point in the simulations, a relatively straightforward algorithm is adopted. In order to maintain the greatest parametric flexibility, the current waveform, $I_\phi(t)$, is specified *a priori* in these simulations, although an option also exists to preprogram the individual coil voltages. An exponential rise of the plasma current, with a characteristic rise-time, τ_R , is used and assumes the form

$$I_\phi(t) = (I_\phi^{MAX} - I_\phi^{MIN})(1 - e^{-t/\tau_R}) + I_\phi^{MIN}, \quad (12.2-18)$$

where typically $I_\phi^{MIN} \simeq 0.2$ MA, and $I_\phi^{MAX} = 10.4$ MA is the ARIES-I steady-state current value.

To properly model the interaction between the plasma and the PF coils during start-up, an equivalent-circuit approach is used. In Fig. 12.2-1, the entire ARIES-I PF-coil set and its locations are displayed. As defined by the output from the equilibrium code, VEQ [15], the 12 coils in the upper half of the plasma cross section are collapsed into six groups as shown. The self- and mutual inductances for any two groups of coils, designated A and B, each with n_A and n_B coils, are given by, respectively

$$L_A = \frac{1}{n_A^2} \left(\sum_{i=1}^{n_A} L_i + \sum_{i=1}^{n_A} \sum_{j=1, j \neq i}^{n_A} M_{ij} \right), \quad (12.2-19)$$

$$M_{AB} = \frac{1}{n_A n_B} \sum_{i=1}^{n_A} \sum_{j=1}^{n_B} M_{ij}, \quad (12.2-20)$$

where L_i is the self-inductance of the i th coil and M_{ij} is the mutual inductance between the i th and j th coils within a coil group. Figure 12.2-2 shows an equivalent circuit for the n ($=6$) collapsed coil sets, for which all the inductances can be computed independently from the VEQ output. The plasma is simply represented as an additional coil with inductance L_p and resistance R_p . An equivalent voltage source, V_{RF} , is used to model the RF current-drive power.

To preserve the plasma equilibrium during start-up, the ratio of the coil current for the i th coil group, I_{gi} , to the plasma current, $I_{gi}/I_\phi = C_i$, is kept constant. Since the plasma current, I_ϕ , is known, each of the C_i constants can be determined from VEQ. This allows decoupling of the plasma circuit equation from the rest of the circuit shown in Fig. 12.2-2. To illustrate this, one can write the plasma circuit equation as

$$-V_{RF} + I_\phi R_p + L_p \frac{dI_\phi}{dt} + \sum_{i=1}^n M_{ip} \frac{dI_{gi}}{dt} = 0, \quad (12.2-21)$$

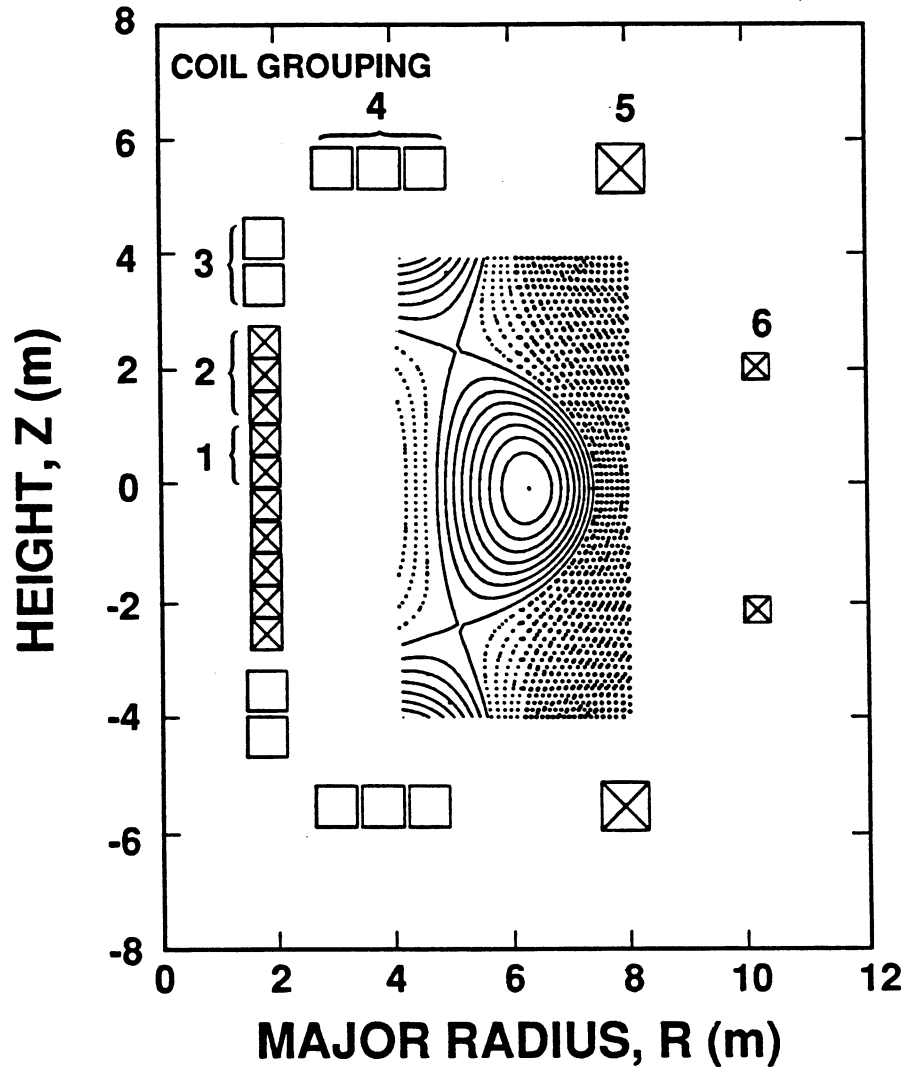


Figure 12.2-1. ARIES-I PF-coil set, as determined by VEQ [15], showing the collapsing of 12 coils into 6 groups.

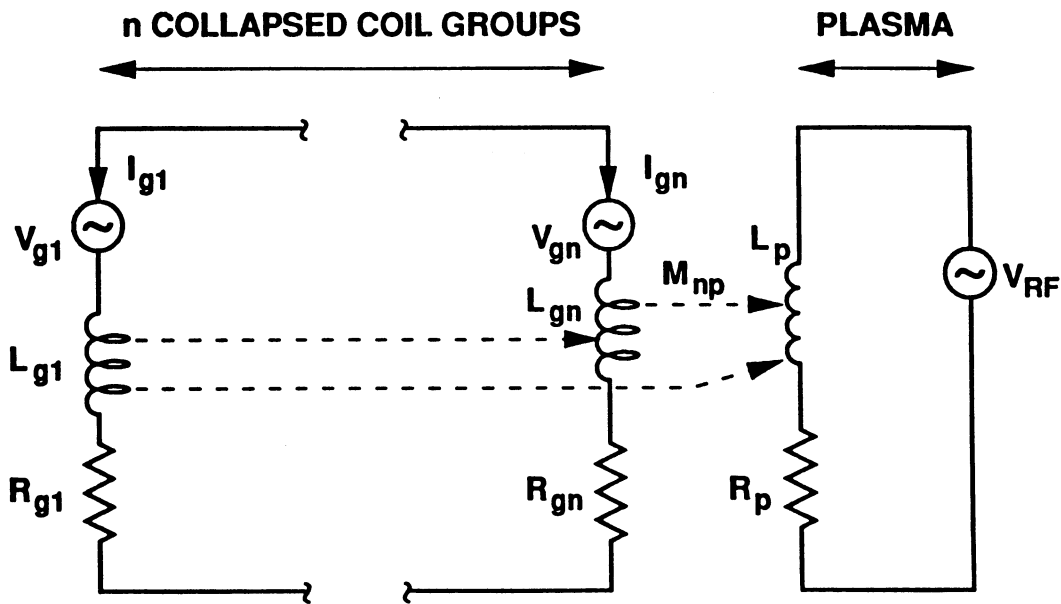


Figure 12.2-2. Equivalent (collapsed) PF-coil set and plasma circuit used in the start-up simulation model.

which reduces to Eq. (12.2-14) if

$$L_E \equiv L_p + \sum_{i=1}^n C_i M_{ip} \tag{12.2-22}$$

and $V_{RF} \equiv I_{RF} R_p$.

12.2.1.4. First-wall model

The ARIES-I first wall is a bank of SiC tubes cooled by helium. A cross section of the start-up code model for the first wall is shown in Fig. 12.2-3. Table 12.2-I lists the main dimensions and physical properties used to assess the thermomechanical response of the first-wall tube bank. In addition, a first-wall evaporation and sputtering model is used to dynamically feed impurities to the plasma. However, because of the relatively low power and particle fluxes and the first-wall materials for ARIES-I, impurity feedback is not an important effect. Details of the first-wall thermomechanical model are given in Ref. [16].

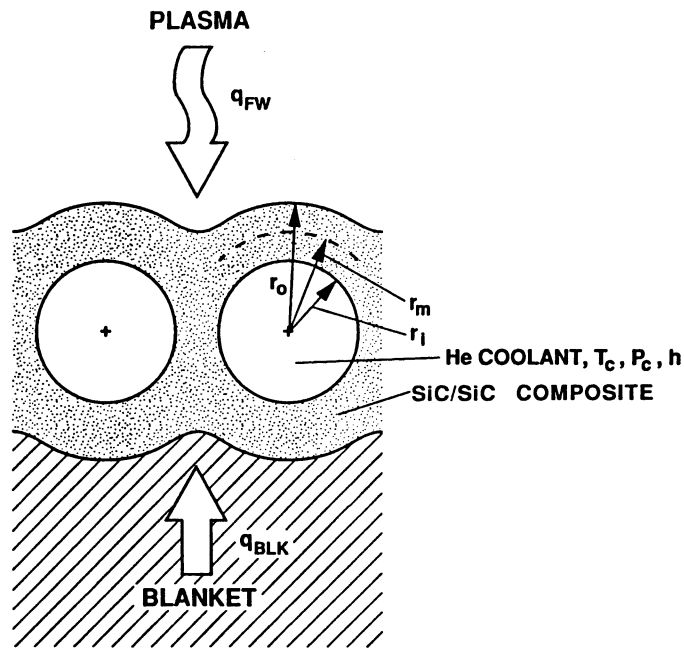


Figure 12.2-3. First-wall model used to estimate the transient thermomechanical response for ARIES-I ($r_i = 4$ mm, $r_m = 5.5$ mm, $r_o = 7$ mm).

Table 12.2-I.
First-Wall Parameters Used in ARIES-I Start-Up Simulations

Density, ρ (kg/m ³)	3,217
Thermal conductivity, κ (W/K-m)	15
Heat transfer coefficient, h (W/K-m ²)	2,198
Heat capacity, c_p (J/K-kg)	1,200
Thermal expansion coefficient, α (10 ⁻⁶ /K)	4.5
Young's modulus, E (GPa)	240
Poisson's ratio, ν	0.30
Inner radius, r_i (mm)	4.0
Midpoint radius, r_m (mm)	5.5
Outer radius, r_o (mm)	7.0
Coolant temperature, T_c (K)	923

12.2.2. Results of Simulations

Start-up transients, based on a combination of inductive and RF current drive, are given for the ARIES-I plasma. Table 12.2-II lists the initial plasma parameters assumed for the simulations. Strictly speaking, these parameters, at the end of current initiation, can be determined by solving the stationary-particle and power-balance equations with a small amount of lower-hybrid input power. However, this approach is not used in this study because the simulation results are found to be relatively insensitive to the initial plasma parameters. The initial plasma density is then chosen by considering the minimum value allowed by the runaway-electron limit and the maximum value governed by the Greenwald limit [17]. This latter density limit, however, is generally violated by $\sim 50\%$ for full-power steady-state conditions and must be re-examined in the context of a DT-burning plasma including the α -particle pressure. The initial plasma beta is constrained to be below the Troyon limit of $C_T = \beta B a / I_\phi \simeq 0.03$. The simulation results presented in this section are grouped as time histories of currents, voltages, powers, and energies in the PF-coil circuit (Figs. 12.2-4 and 12.2-5), profile-averaged plasma properties (Fig. 12.2-6), and plasma powers (Fig. 12.2-7).

As noted in Sec. 12.2.1, all start-up simulations for ARIES-I assume *a priori* that the plasma current follows an exponential rise with a rise-time, τ_R , described by Eq. (12.2-18), and calculates the required programming of the PF-coil voltages and powers. During the lower-hybrid-driven current-ramp phase, the plasma is fueled at a rate that is 5% above

Table 12.2-II.
Initial Plasma Conditions Used in ARIES-I Start-Up Simulations

Plasma current, I_ϕ^{MIN} (MA)	0.2
Density-weighted average temperature, $T_{i,e}$ (keV)	0.4
Average density, $n_{i,e}$ (m^{-3})	1.1×10^{19}
Dreicer parameter, $E_{ }/E_D$	0.01
Volume-averaged beta, β_ϕ	3.13×10^{-6}
Plasma-current ramp time, τ_R (s)	600
Effective charge, Z_{eff}	1.45

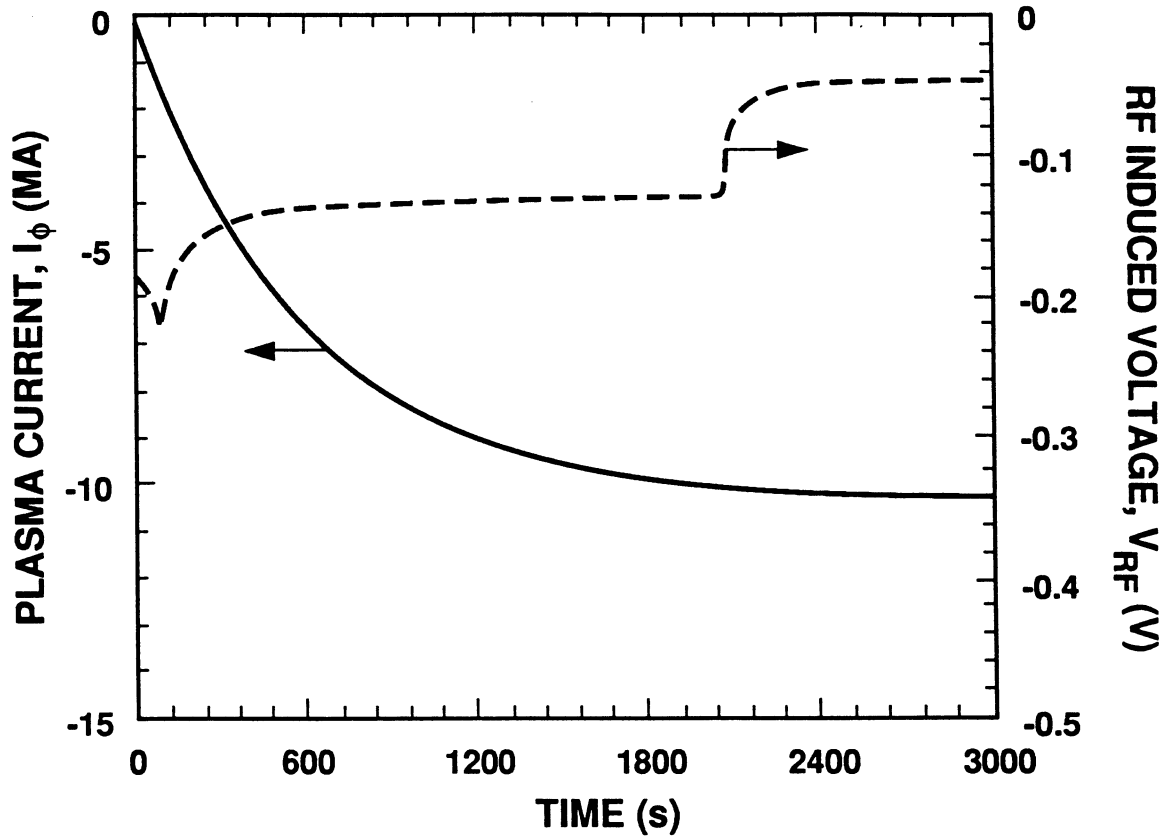


Figure 12.2-4. Transient response of the plasma current and RF voltage for the ARIES-I reference start-up scenario.

the particle loss rate which is characterized by $\tau_p = 4\tau_E$. To maximize the current-drive efficiency, the initial ion density, n_{iR} , is kept low at $n_{iF}/n_{iR} \approx 1 - 10$, where n_{iF} is the steady-state value. At $t = 3.5\tau_R$, when $I_\phi/I_\phi^{MAX} \simeq 0.97$, the fueling rate is increased in a controlled fashion to allow the plasma to follow the remaining current transient to its steady-state design conditions. At the same time, fast-wave power is switched on to maintain the current and to provide auxiliary heating to the plasma. Extensive parametric studies have been carried out for these start-up scenarios using τ_R (characteristic rise-time of plasma current) and n_{iF}/n_{iR} (ratio of steady-state final density to that of the current ramp-up phase) as variables, primarily to assess the lower-hybrid and fast-wave power requirements for a reasonable start-up time. In most of the cases studied, the gas fueling assumes a 50:50 DT mixture. However, to protect the divertor plates during these power transients, ramp-up of the plasma density to its full value should be as quick as is practical, while the fusion power level is controlled by adjusting the composition of the

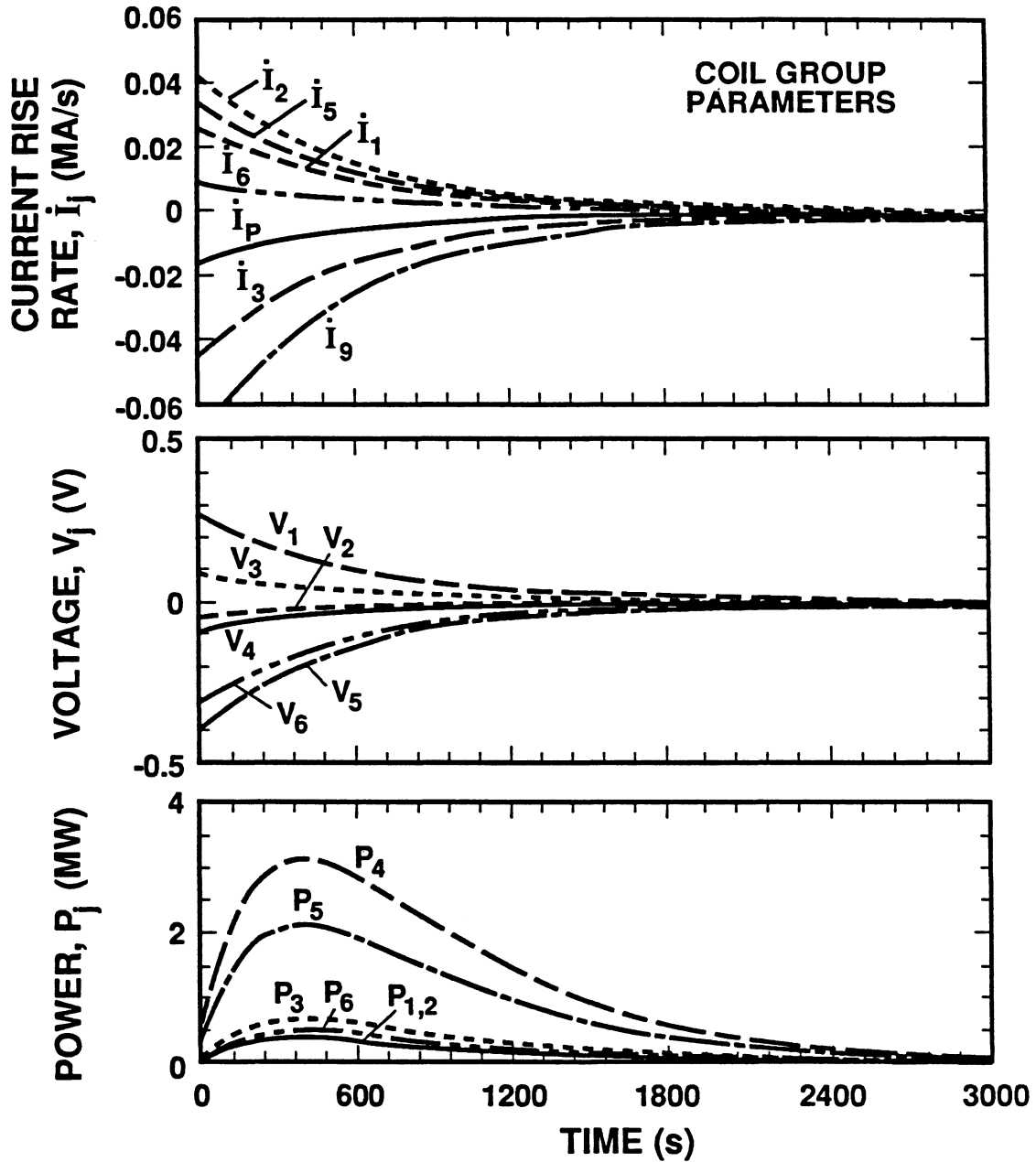


Figure 12.2-5. Transient response of the PF-coil circuit for the ARIES-I reference start-up scenario showing the current rise rate, coil voltage, and coil input power.

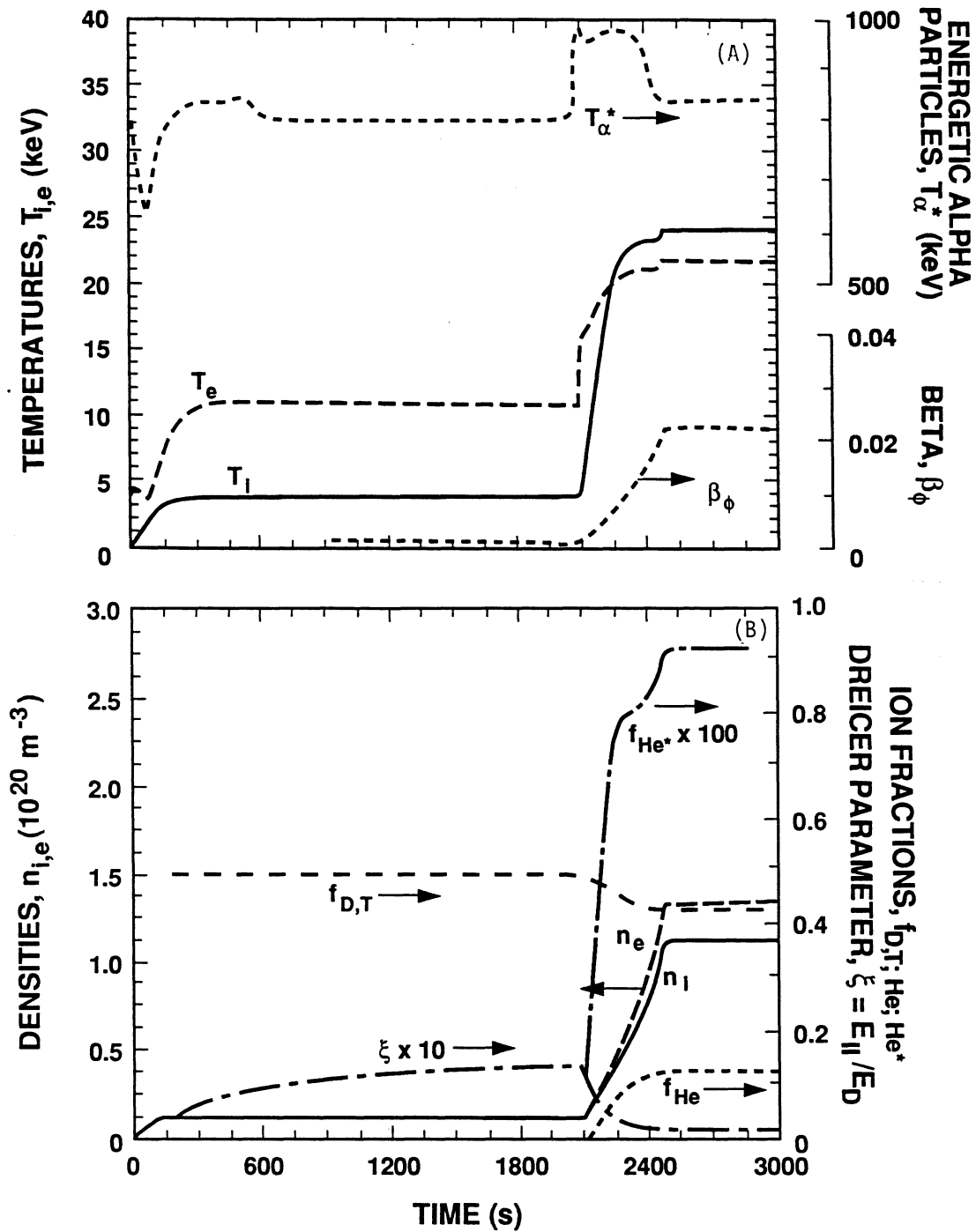


Figure 12.2-6. Transients of ARIES-I plasma parameters during the reference start-up scenario: (A) Electron and ion temperatures, energetic α -particle temperature, and plasma β ; (B) Electron and fuel ion densities, various ion fractions, and Dreicer parameter (He^* and α^* represent energetic α particles).

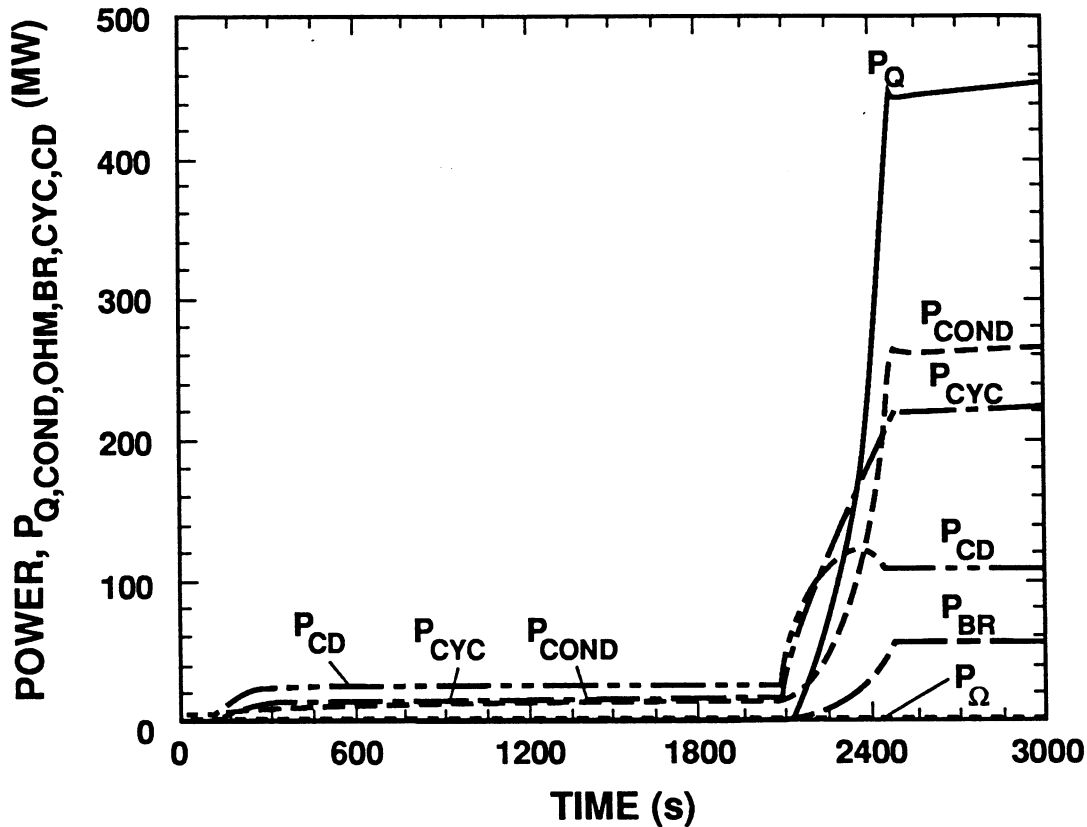


Figure 12.2-7. Transient response of various plasma power components in the reference ARIES-I start-up scenario: α -particle heating power (P_Q), transport power loss (P_{COND}), ohmic dissipation (P_Ω), bremsstrahlung (P_{BR}) and synchrotron (P_{CYC}) powers, and current-drive heating (P_{CD}).

DT fuel mixture. This control technique admits the possibility of a rapid density rise and a slower power transient with a tritium-lean fuel mixture. Scenarios involving this feature are also examined in the simulations and are presented in Sec. 12.2.2.4.

12.2.2.1. Reference case study

The temporal response of the ARIES-I plasma-coil circuit to a plasma-current waveform given by Eq. (12.2-18) is studied first. This reference ARIES-I case uses $\tau_R = 600$ s and initial plasma parameters given in Table 12.2-II. Specifically, the following initial values are assumed: $I_\phi^{MIN} = 0.2$ MA, $n_{iR} = 1.1 \times 10^{19} \text{ m}^{-3}$ for an assumed $n_{iF}/n_{iR} = 10$, and $T_i = 0.4$ keV. In Fig. 12.2-4, the time evolution of the plasma current, I_ϕ , and RF current-drive voltage, V_{RF} , is displayed. The rapid drops of V_{RF} at $t \simeq 100$ s and $t = 2000$ s reflect mainly a decrease in R_p due to a rise in electron temperature, T_e , at

these points, as shown in Fig. 12.2-6(A). In Fig. 12.2-5, the coil current-rise rates, coil voltages, and input powers to the six PF-coil groups are given. The current and voltage transients in this case are well within the design limits of the PF-coil system.

The time evolution of the relevant plasma parameters during the entire reference start-up phase for ARIES-I is also shown in Fig. 12.2-6. Specifically shown in Fig. 12.2-6(A) are the density-weighted volume-averaged electron and ion temperatures, respectively, T_e and T_i , and the total plasma beta, β_ϕ , as a function of time. During the low-density current-ramp phase ($0 \leq t \leq 2100$ s), $T_e \gg T_i$ because all the lower-hybrid power (~ 20 MW) is absorbed by electrons that are essentially decoupled from the fuel ions. At $t = 2100$ s, rapid density ramp-up occurs while the fast-wave power is raised to its full value in a controlled fashion. The steady-state conditions prescribed for ARIES-I are attained at $t \simeq 2500$ s. In Fig. 12.2-6(B), the density evolution and the ion-species fractions, including those of thermal and energetic α -particles, are displayed. The time variation of the Dreicer parameter, $\xi (= E_{\parallel}/E_D)$, is also shown. In this case, the value of ξ peaks at the end of the current ramp and is ~ 0.01 , barely within the runaway limit.

Figure 12.2-7 gives the time evolution of the various power terms in the plasma power-balance equations for the ARIES-I reference start-up scenario. These include the α -particle heating power, the transport power loss, the ohmic dissipation, the synchrotron and bremsstrahlung powers, and the current-drive power, P_{CD} . The P_{CD} curve represents the programmed RF-power waveform that is needed to ramp up and sustain the current during the entire plasma start-up phase. In this reference case, the lower-hybrid current-drive power requirement for the low-density current ramp-up is found to be modest (≤ 20 MW). For $t \geq 2100$ s, the increase in P_{CD} reflects the changeover to FWCD. As discussed in Sec. 12.2.1, the synchrotron power is comparable to the transport power throughout the entire start-up and bremsstrahlung radiation losses are much smaller.

12.2.2.2. First-wall response

The thermal and mechanical responses of the ARIES-I first wall to the reference start-up scenario were also analyzed. The following relevant first-wall power densities are computed in the code: (A) neutron wall loading, I_w ; (B) radiated heat flux, $q_{RAD} = [P_{BR} + P_{LINE} + P_{CYC}/(1 - f_H)]/A_{FW}$, where P_{LINE} is the line radiation power, f_H is the first-wall hole fraction, and A_{FW} is the nominal first-wall surface area; and (C) maximum total heat flux, $q_{TOT} = (P_Q + P_\Omega + P_{CD})/A_{FW}$. In principle, q_{RAD} should be used to estimate the first-wall thermomechanical transient behavior under the assumption that the divertor is operating during start-up. However, in order to examine a

worst-case scenario (no divertor operation), q_{TOT} is used instead in the code calculations (all plasma power appearing on the first wall). In Fig. 12.2-8(A), the 1-D thermal response of the ARIES-I first wall (Fig. 12.2-3), accounting for one-sided surface heat flux, is given. In particular, the temperatures of the coolant tube at the outer, middle, and inner radii are displayed. The neutron wall loading, I_w , and heat fluxes, q_{RAD} and q_{TOT} , are plotted as functions of time in the lower half of Fig. 12.2-8(B). In the same figure, the transient mechanical response of the first wall is shown in terms of the secondary (thermal) stress, σ_θ , at the inner and outer tube radii. The primary (pressure) stress, σ_θ^p , for the ~ 10 -MPa He coolant gives rise to loop components of 9.7 and 19.7 MPa at, respectively, the inner and outer tube radii. These stress levels appear to be well within the design limits for the SiC coolant-tube structures. A more detailed treatment of the thermomechanical behavior of the first wall at steady state is given in Sec. 8.3.2.

12.2.2.3. Parametric studies

In the start-up simulation results reported up to this point, τ_R has been fixed at 600 s and the density is kept at the low value of $1.1 \times 10^{19} \text{ m}^{-3}$ (*i.e.*, $n_{iF}/n_{iR} = 10$) during the current ramp-up phase. In addition, a series of parametric calculations have been carried out with respect to variations in the prescribed current rise-time and the density at the ramp-up phase (see Fig. 12.2-9) in order to study their impact on the maximum-required current-drive power, P_{CD}^{MAX} , and the plasma evolution. Figure 12.2-9(A) depicts the influence of varying τ_R on the current-drive program to reach the steady state for a fixed ratio of $n_{iF}/n_{iR} = 10$ and the initial parameters shown in Table 12.2-II. As τ_R is decreased from 600 s, \dot{I}_ϕ increases throughout the early phase of the current ramp-up. Noting that $P_{CD} \propto I_{RF} = I_\phi + (L_E/R_p)\dot{I}_\phi$, and that R_p decreases as electrons are heated during the start-up, a maximum in P_{CD} occurs. As an extreme example, a P_{CD}^{MAX} of 340 MW is needed to achieve an exponential rise-time of 150 s for the plasma current. In Fig. 12.2-9(B), the corresponding plasma temperature evolution is shown for $\tau_R = 150$ s, 200 s, and 600 s. For the cases with $\tau_R < 600$ s, a temperature excursion in electrons is observed in the initial phase of the current ramp-up because of the strong ohmic heating of electrons from the rapid current rise. In the extreme case of $\tau_R = 150$ s, T_e peaks beyond 40 keV while T_i reaches a maximum value of 10 keV, resulting in significant α -particle production in the 50:50 DT mixture used. Excursions in T_e to above ~ 15 keV prevent core penetration of the lower-hybrid waves and must be avoided.

Start-up simulations have also been performed using ARIES-I parameters for various values of n_{iF}/n_{iR} at $n_{iF} = 1.1 \times 10^{20} \text{ m}^{-3}$ and $\tau_R = 600$ s, and the results are displayed

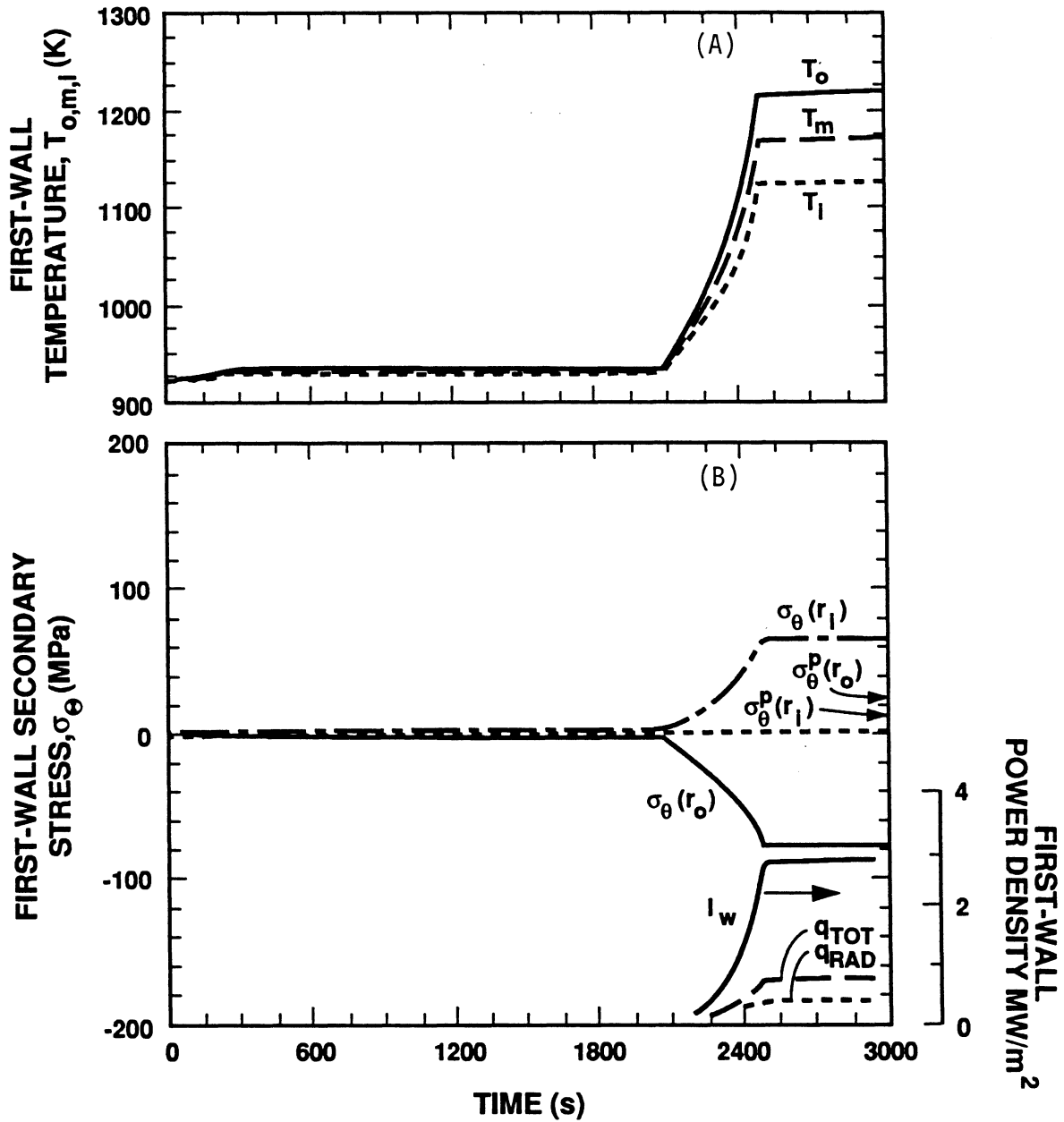


Figure 12.2-8. Transient thermal and mechanical responses of ARIES-I first wall for reference start-up scenario: (A) Coolant tube temperatures (T_i , T_m , and T_o at, respectively, inner, mid and outer radii); (B) Neutron wall loading (I_w), heat fluxes (q_{RAD} and q_{TOT}), secondary (thermal) stresses [$\sigma_\theta(r_i)$ and $\sigma_\theta(r_o)$], and primary (pressure) stress [$\sigma_\theta^p(r_i)$ and $\sigma_\theta^p(r_o)$] (r_i and r_o denote, respectively, inner and outer tube radii).

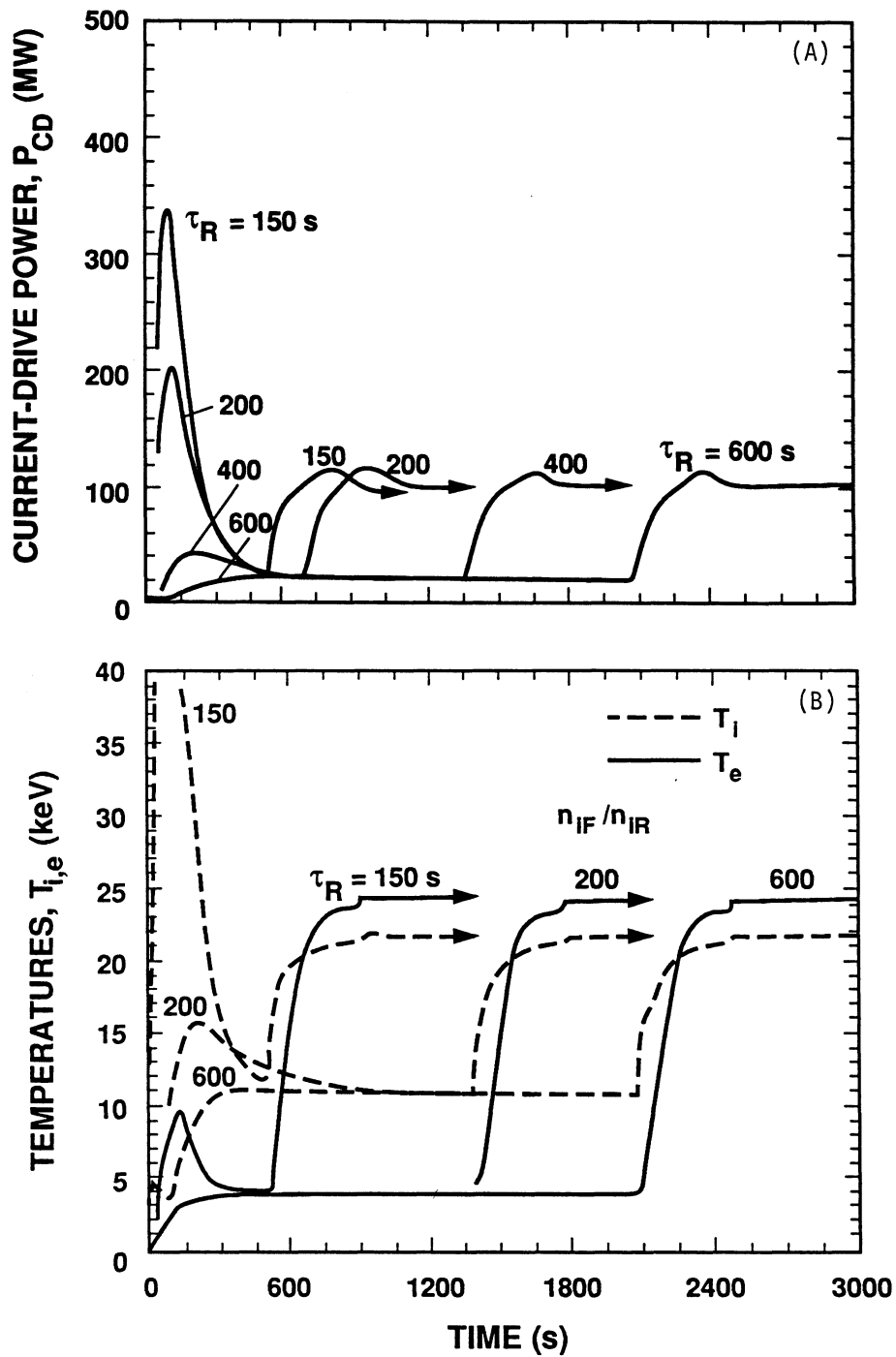


Figure 12.2-9. Plasma transient response for start-up scenarios with $\tau_R = 150$ s, 200 s, 400 s, and 600 s, at $n_{iF}/n_{iR} = 10$: (A) Current-drive power, and (B) Ion and electron temperatures.

in Fig. 12.2-10 as time histories of T_i and T_e . At higher values of n_{iR} , more lower-hybrid power is required to achieve the same current ramp rate because the current-drive efficiency is inversely proportional to n_e . These larger current-drive (and heating) powers lead to higher temperatures and, in some cases, substantial α -particle production in the current ramp-up phase. Again, for these “high-density” start-up scenarios, the question of penetration of the lower-hybrid wave power to the plasma core warrants a more careful study.

The results of these parametric studies are summarized in Fig. 12.2-11. Here, P_{CD}^{MAX} for the lower-hybrid current-ramp phase is plotted as a function of τ_R at $n_{iF}/n_{iR} = 10$, and also as a function of n_{iF}/n_{iR} at $\tau_R = 600$ s. For both cases, $n_{iF} = 1.1 \times 10^{20} \text{ m}^{-3}$. For reasons given previously, P_{CD}^{MAX} decreases with increasing τ_R and n_{iF}/n_{iR} . Also

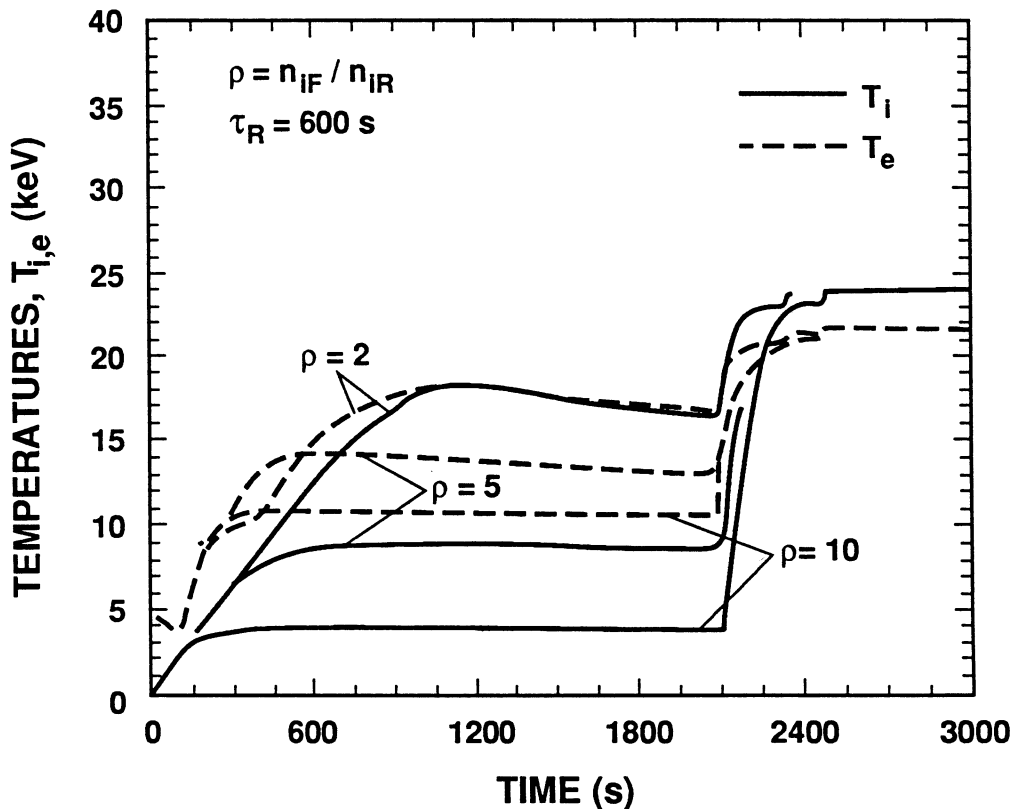


Figure 12.2-10. Time evolution of plasma temperatures in ARIES-I start-up simulations with $\tau_R = 600$ s and $n_{iF}/n_{iR} = 2, 5,$ and 10 .

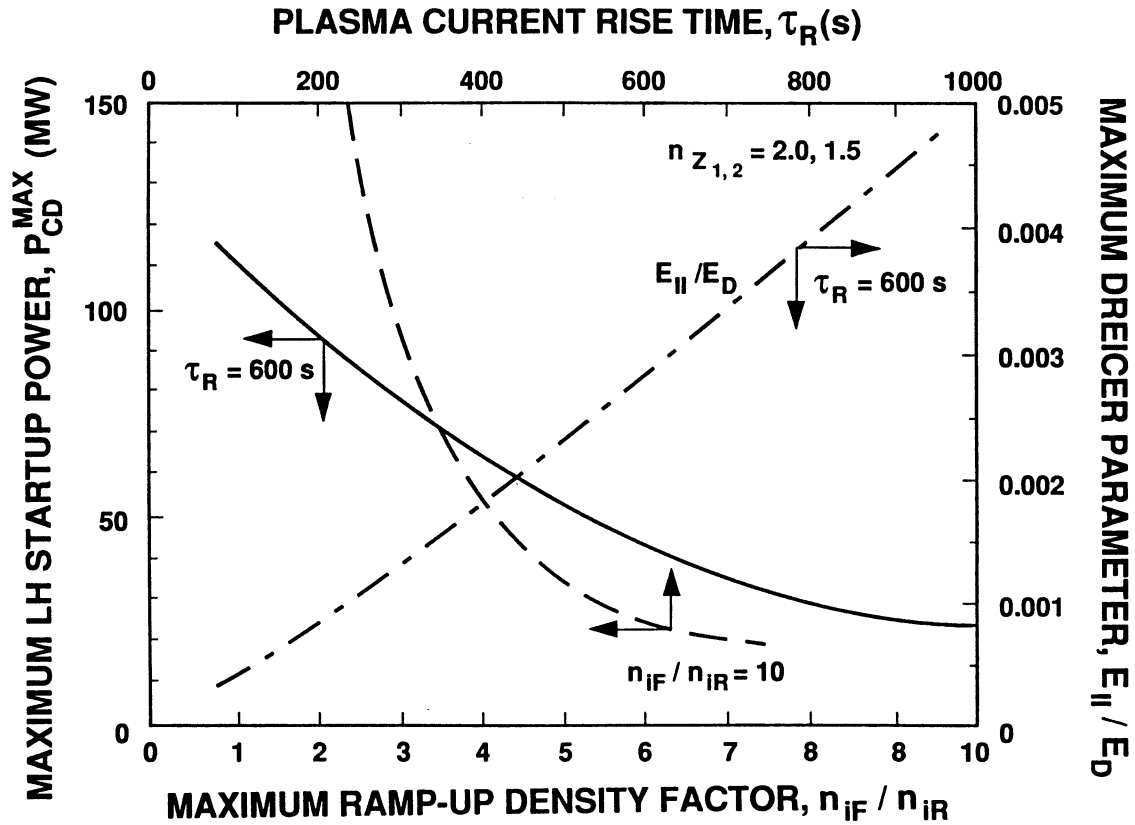


Figure 12.2-11. Dependence of maximum current-drive power during current ramp-up phase on current rise-time for $n_{iF}/n_{iR} = 10$, and on n_{iF}/n_{iR} for $\tau_R = 600$ s, using ARIES-I reference parameters in Table 12.2-II. The maximum Dreicer parameter is also displayed as a function of n_{iF}/n_{iR} for $\tau_R = 600$ s.

plotted in Fig. 12.2-11 is the maximum value of the Dreicer parameter, ξ , as a function of n_{iF}/n_{iR} at $\tau_R = 600$ s. The linear rise of the Dreicer parameter with n_{iF}/n_{iR} can be deduced by noting that

$$|E_{||}^{MAX}| = \frac{L_E}{2\pi R_T} [\dot{I}_\phi]_{MAX}, \quad (12.2-23)$$

where $[\dot{I}_\phi]_{MAX}$ is determined by τ_R through Eq. (12.2-18), and by using the definition of E_D in Eq. (12.2-16). It can be shown easily that lowering τ_R from 600 s raises the curve for ξ vertically in the figure and violates the $\xi \leq 0.01$ runaway condition at higher values of n_{iF}/n_{iR} . Therefore, in order to minimize the lower-hybrid power requirement and achieve a reasonable current rise-time while avoiding runaway-electron effects, the reference case presented in Sec. 12.2.2.1 appears to be an appropriate choice for ARIES-I plasma start-up.

12.2.2.4. Control of power ramp-up

As noted in Sec. 12.2.2, with the full plasma current set at low density, protection of the divertor plates may require the rapid establishment of the operating plasma density as the fusion power is ramped up at a slower rate to its steady-state level. This start-up feature also offers the additional advantage of minimizing the power transients on the blanket, primary coolant, steam generator, and turbine systems. To achieve this, a density ramp-up scenario using a variable DT fuel mixture can be considered. The range of possibilities in this context would be defined by the 50:50 DT transients studied in Secs. 12.2.2.2 and 12.2.2.3, and those of a near 100% deuterium (99:1 DT) mixture. The resulting temperature and power transients for these two start-up scenarios are shown in Fig. 12.2-12, using the reference ARIES-I parameters of Table 12.2-II. In Table 12.2-III, the steady-state powers at the end of the two start-up scenarios are compared. Relative to the case of 50:50 DT start-up, the $\sim 100\%$ deuterium start-up reduces the neutron and the charged particle powers by factors of, respectively, 25.6 and 21.2. However, because the current-drive power is increased by a factor of 2.4 due to the lower T_e and because the radiation power loss is smaller, the heat flux to the divertor plates is reduced by only 50%. The requirement of 244 MW of fast-wave power to drive the current in the deuterium start-up case is clearly unacceptable for ARIES-I since only about 100 MW of FWCD power is prescribed for steady-state operation. A lower FWCD power for this case is possible in principle, with a somewhat lower target density prior to the injection of tritium.

A more elaborate power ramp-up scheme involving feedback control of the density fueling rate can also be considered. The key is to maintain the FWCD power to below ~ 100 MW during the fusion-power ramp phase under the constraint

$$\frac{\gamma_{FW} P_{CD}}{n_e(1 - f_{BS})} = I_\phi, \quad (12.2-24)$$

where γ_{FW} and f_{BS} are given by, respectively, Eqs. (12.2-17) and (12.2-9) and $I_\phi \simeq 10$ MA in the reference case. The density is dictated by the fueling rate while the temperature can be partially controlled by the fuel mixture. Partial-power operation, demanded by engineering constraints during start-up, is relatively straightforward (using passive burn-control techniques involving density and auxiliary heating power) as long as the plasma is operating in a thermally stable region. However, in regions of low temperatures ($< 10\text{--}15$ keV) where the plasma is thermally unstable, active feedback control will be needed. Because the ARIES-I reactor is based on steady-state current drive, a more detailed analysis is needed to assess the impact of the requirement of partial-power

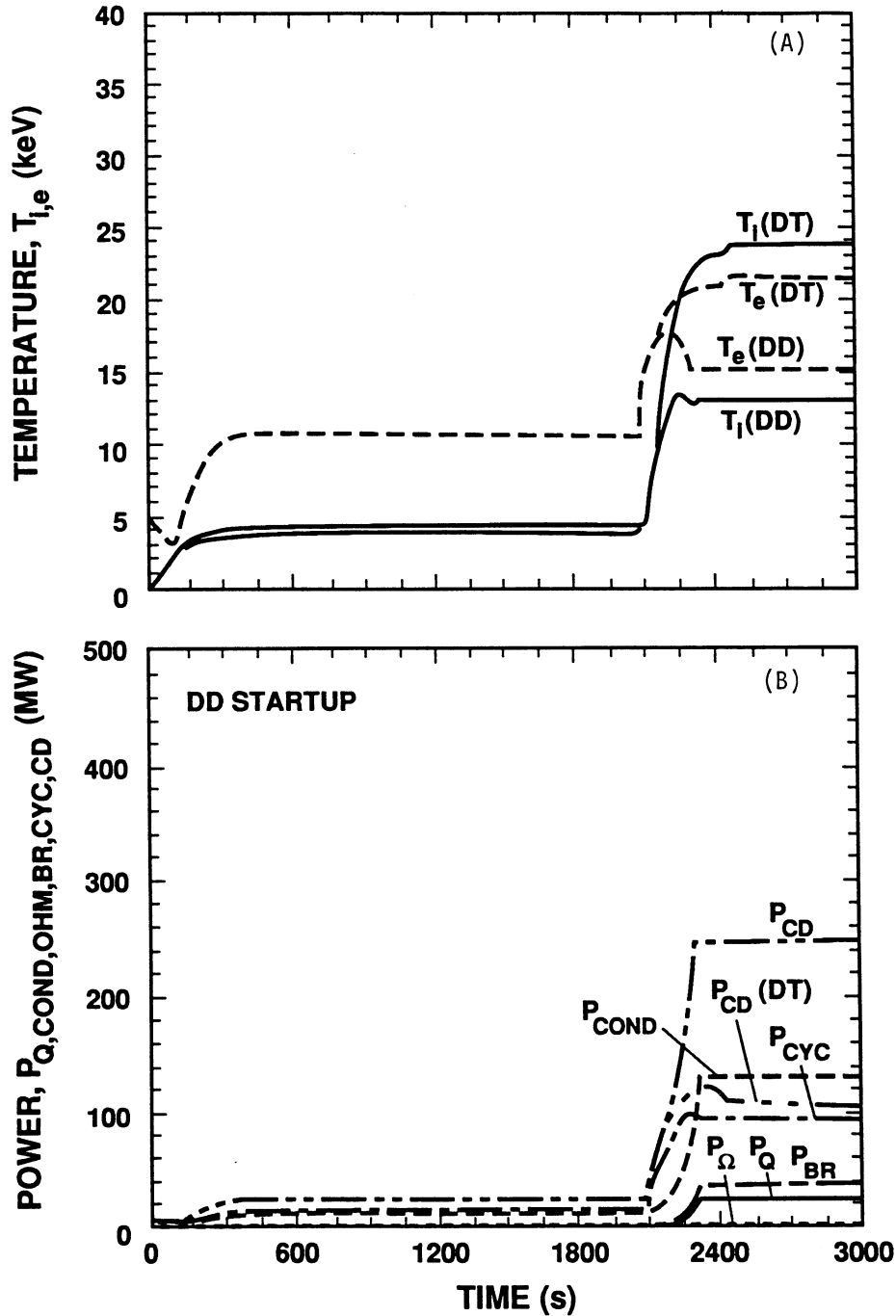


Figure 12.2-12. Comparison of plasma transients between ARIES-I start-up scenarios with 50:50 and 99:1 DT fuel mixtures: (A) Plasma temperatures, and (B) Plasma powers for the 99:1 DT case and P_{CD} for the 50:50 DT case [α -particle heating power (P_Q), transport power loss (P_{COND}), ohmic dissipation (P_Ω), bremsstrahlung (P_{BR}) and synchrotron (P_{CYC}) powers, and current-drive heating (P_{CD})].

Table 12.2-III.
Steady-State Powers for DT and DD Start-Up

DT Fuel Mixture	Systems Code	Start-Up Model	
	50:50	50:50	99:1
Electron temperature, T_e (keV)	19.3	27.6	15.1
Ion temperature, T_i (keV)	20.0	21.6	12.0
Total thermal power, ^(a) P_{TH} (MW)	2,026.9	2,325.9	361.5
Fusion power, P_F (MW)	1,925.4	2,224.4	90.5
Charged particle power, P_Q (MW)	386.7	447.0	21.1
Neutron power, P_n (MW)	1,538.7	1,777.4	69.4
DT neutron, P_{nDT} (MW)	1,538.7	1,775.8	67.1
DD neutron, P_{nDD} (MW)	—	1.6	2.3
FWCD power, P_{CD} (MW)	96.7	101.5	243.8
Transport power, P_{COND} (MW)	244.4	259.0	126.0
Electron, P_{CONDe} (MW)	—	167.9	86.2
Ion, P_{CONDi} (MW)	—	91.1	32.9
Ohmic power, P_Ω (MW)	0.9	0.6	0.8
Bremsstrahlung power, P_{BR} (MW)	45.2	53.2	39.9
Line radiation power, P_{LINE} (MW)	—	19.9	16.4
Cyclotron radiation power, P_{CYC} (MW)	194.7	216.7	90.2
Neutron wall loading, I_W (MW/m ²)			
DT (14.06 MeV)	2.5	2.9	0.1
DD (2.46 MeV)	2.0×10^{-3}	2.2×10^{-3}	3.8×10^{-3}
Plasma Q -value, $Q_p = P_F/P_{RF}$	19.9	22.8	1.2

^(a)Without neutron energy multiplication.

operation on the overall design. Safe operation of the divertor during the start-up and partial-power phases should also be studied.

12.2.3. Summary and Critical Issues

A simple 0-D plasma-circuit code has been used to study start-up scenarios for ARIES-I. About 20 MW of lower-hybrid power is required to ramp up the current to its full value at low density ($\simeq 1.1 \times 10^{19} \text{ m}^{-3}$) in about 2100 s. At nearly full current, the fuel ion density is raised quickly by enhanced fueling with a 50:50 DT mixture while the FWCD power of ~ 100 MW is applied. This fusion-power ramp-up phase lasts for about 400 s. The final plasma parameters predicted by the start-up simulation generally agree well with the steady-state predictions of the ARIES systems code as outlined in Table 12.2-III. Some of the discrepancies arise from differences in the assumed radial density and temperature profile exponents, α_n and α_T . The ARIES-I strawman design assumes a “pedestal” density profile with $\alpha_n = 1.0$, whereas the start-up simulations use a parabolic profile with $\alpha_n = 0.3$ in order to best match the fusion reactivity profile factor, α_{DT} . Differences in α_{DT} (7% less in the start-up model), coupled with those in temperature (24 keV *vs* 20 keV, giving a 30% difference in $\langle\sigma v\rangle_{DT}$) and the final fuel density (5% less in the start-up simulation), account for the $\sim 15\%$ difference (increase) in the steady-state fusion power predicted by the start-up model. Although fine tuning the code should bring the start-up and systems models into better alignment, the present agreement is considered adequate for the purpose of this study.

It is noted that the simulation results reported in this section represent only a preliminary assessment of a plausible start-up scenario for ARIES-I. In addition to examining the impact of longer current-rise times on reducing the start-up power requirement, ways to better utilize the inherent volt-second capability of the PF-coil set should be investigated [15]. Other important features of the start-up scenario also remain to be examined. In particular, scenarios involving slower fusion-power ramp-up may be desirable from the viewpoint of safe operation of the steam generator and turbine systems, while divertor protection may require a more rapid density buildup. In order to satisfy both of these needs, a tritium-lean fueling scenario followed by a slower, full-density power ramp-up may be required. However, the feasibility of this scheme under the constraints of steady-state ARIES-I power requirements remains to be shown.

12.3. PLANT START-UP

Operating constraints of the various phases of the plasma and current start-up for the ARIES-I reactor were examined in detail in Sec. 12.2. Likewise, the engineering aspects of ARIES-I will also place constraints on the start-up and partial- and over-power operations of the reactor plant. These constraints are due to the temperature and thermal stress limits of the first-wall, blanket, divertor, and power-conversion system materials, and to the power requirements for magnet cool-down, blanket heat-up, and coolant circulation. In Sec. 12.3.1, the plant start-up procedure and the associated constraints imposed on the reactor subsystems are outlined. Section 12.3.2 gives an assessment of the range of operating parameters for the various plant components under the conditions of partial- and over-power operations. The time scale of power ramp-up imposed by these engineering considerations can in general be met by careful control of the plasma start-up.

12.3.1. Start-Up Requirements

To start up the ARIES-I fusion-power reactor will require a number of actions involving the engineering systems:

- Cool down and energize the superconducting magnets.
- Heat up and pressurize the primary coolant and power conversion systems.
- Initiate the plasma operations at low power.
- Balance the power-conversion-system conditions for power operation.
- Roll the turbines and synchronize with the grid.
- Increase the plasma power and load the turbines to minimum stable power levels (about 10% of full power).
- Ramp up the plasma and power conversion system to full power.

Each of these steps requires some time to accomplish and has the potential for imposing engineering constraints.

The cool-down and energizing of the superconducting magnets will be governed by the power limits of the helium refrigeration system and the magnet-current power supply.

With the present ARIES-I systems, cool-down and energizing would take approximately one week. This could be reduced significantly, if desired, by simply providing larger refrigeration and power supply systems. Since the magnets will not be de-energized, much less warmed up, for routine shutdowns, the added expense of larger systems is not justified. The coils will be warmed only when they are to be removed for annual (at most) blanket replacement.

Heat-up of the blanket, the primary coolant circuit, and the power conversion system will be done with the main helium circulator pumps (~ 20 MW) run at 100% power, based on HTGR experience [18], and will take about three hours. At this point, plasma heating will be initiated using the fast-wave current-drive and heating system (~ 100 MW) to bring the plant to $\sim 10\%$ thermal power and to balance the power conversion system.

In a conventional power plant, steam turbines are massive structures with much longer thermal time constants than other components, such as the steam generator. Therefore, the start-up time is primarily the time needed to slowly heat the turbines to the operating temperature while staying within the thermal stress limit. Plants with an advanced steam cycle have longer start-up times because more time is needed to complete the temperature ramp to the higher throttle temperature required by the advanced design. Table 12.3-I shows the start-up times from two previous studies [19, 20] for a bare plant (presently operating) and an advanced plant using an advanced steam cycle similar to that proposed for ARIES-I. The longest time for cold start-up is expected to be about 10

Table 12.3-I.
Start-Up Times (h) for Coal-Fired Power Plants

Type of Start-Up	Westinghouse [19]		General Electric [20]	
	Bare Plant	Advanced Plant	Bare Plant	Advanced Plant
Cold	9.1	9.9	8.1	10.
After weekend shutdown	—	—	3.6	5.5
Warm	~ 2.0	~ 2.4	—	—
Hot	~ 1.4	2.0	—	—

hours when the operating parameters of the system (temperature and pressure) attain their design values. This is accomplished at about 10% of full power. Start-up after weekend shutdown requires about six hours, and warm or hot start-up takes about two hours. A steam generator can be loaded at 2% per minute, so unloading during shutdown can be done at about 1% per minute. The plant is generally tripped at 10% of full power.

The plasma start-up time is on the order of tens of minutes for ARIES-I, as mentioned in the previous section. The thermal time constants of the first wall, blanket, and divertor are very short, on the order of seconds. Therefore, it is the start-up time for the power conversion system that determines the start-up time of ARIES-I. With the magnets already energized, the total start-up time from cold and hot shutdowns to full power will be, respectively, about twelve and two hours. The orderly shutdown time will be nearly two hours.

12.3.2. Partial- and Over-Power Operations

Based on the configuration of the ARIES-I reference outboard first-wall and blanket designs, calculations were performed to estimate the range of equilibrium partial- and over-power operations that would be permitted without exceeding any of the design limits of the first-wall and blanket materials. Three design criteria were used for the evaluation:

- The SiC-composite-material maximum temperature should be $< 1100^{\circ}\text{C}$,
- The Li_2ZrO_3 operating temperature should be designed to be within the temperature window of 400 to 1400°C , and
- Structural and thermal stresses have to be designed to SiC-composite-material design limits.

In summary, the results of this analysis show that the maximum-acceptable wall loading is defined by the SiC-composite maximum-allowable temperature; the minimum-acceptable wall loading is defined by the minimum-allowable temperature of the solid breeder. The bases for these design limits are presented in Sec. 8.

Table 12.3-II shows the operating parameters of the maximum wall-loading case compared to the reference design at the mid-plane location of the outboard blanket. As shown, the maximum wall loading could be as much as 1.9 times that of the reference design. As the wall loading increases, in order to maintain the same coolant inlet and

Table 12.3-II.
Maximum Wall-Loading and Reference Design Parameters

	Maximum Wall Loading	Reference
Neutron wall loading (MW/m ²)	7.35	3.87
Surface wall loading (MW/m ²)	1.16	0.61
First-wall parameters ^(a)		
Heat transfer coefficient (W/K-m ²)	3,690	2,208
Coolant and solid interface temperature (°C)	978	938
Solid maximum temperature (°C)	1,096	1,001
Pressure drop (kPa)	62.1	20.2
Pumping power (MWe)	111	19

^(a)At the outboard mid-plane location.

outlet temperatures, the coolant mass-flow rate will have to be increased. This will increase the heat transfer coefficient at the expense of higher pressure drop and much higher pumping power. The maximum wall temperature will approach the design limit of 1100°C when the wall loading reaches 7.35 MW/m². At this point, the increased thermal stress across the first wall will have reduced its stress design margin to essentially 1.0, but the structural design limits will not yet have been exceeded.

Table 12.3-III shows the operating parameters of the minimum wall-loading case compared to the reference design at the top or bottom location of the second breeder zone. As shown, the minimum wall loading can be as low as 0.1 times that of the reference design before the Li₂ZrO₃ lower operating-temperature limit is reached. This is partly due to the relatively high coolant-inlet temperature of 250°C. As the wall loading decreases, in order to maintain the same coolant inlet and outlet temperatures, the coolant mass-flow rate will have to be decreased. This will drive the coolant to laminar flow and reduce the heat transfer coefficient and the pressure drop. The minimum breeder temperature will reach the lower operating limit of 400°C when the wall loading reaches 0.25 MW/m².

Table 12.3-III.
Minimum Wall-Loading and Reference Design Parameters

	Minimum Wall Loading	Reference
Neutron wall loading (MW/m ²)	0.25	2.48
Surface wall loading (MW/m ²)	0.04	0.391
Breeder zone parameters ^(a)		
Heat transfer coefficient (W/K-m ²)	269	1,989
Reynolds number	1,185	11,848
Coolant and solid interface temperature (°C)	402	460
Solid maximum temperature (°C)	411	544
Pressure drop (kPa)	0.07	4.17
Pumping power (MWe)	0.03	19

^(a)At 2nd breeder zone located at the top or bottom of the outboard blanket and at the coolant-inlet location.

These results indicate that at equilibrium, the ARIES-I reference blanket design allows a large range (from 10% to 190% of the reference design operation) of partial- and over-power operation. Operation at the 190% point is not a practical option because this would leave no design margins for local peaking factors, *etc.* Further, in order to take advantage of the potential for over-power operation, an oversized helium circulator would be required because the pumping power goes up significantly with increasing fusion power. Similarly, the entire power-conversion system would have to be designed with excess capacity. Nevertheless, the wide range of blanket operation that is theoretically possible is an indication of the tolerance for off-nominal operating conditions that the use of the high-temperature, SiC-composite blanket materials provides.

12.4. SUMMARY AND CONCLUSIONS

The plasma physics aspects of the start-up and operation of the ARIES-I reactor have been investigated in detail. Using a 0-D plasma-circuit code, a plausible start-up scenario going from current initiation to steady state has been determined. About 20 MW of lower-hybrid power is required to ramp up the plasma current to its full value at low density ($\simeq 1.1 \times 10^{19} \text{ m}^{-3}$) in 2100 s at a characteristic rise-time of 600 s. Another 400 s is required to raise the density and fusion power to their steady-state levels using FWCD power of ~ 100 MW. Other lower-hybrid power and fueling strategies are possible and will be the subject of future work to further reduce the start-up power requirement while simultaneously meeting a range of plasma constraints.

There appears to be no major R&D issue related to lower-hybrid current ramp-up and current drive specific to ARIES-I since the relevant data base is already well developed. However, the start-up transient codes should be improved by incorporating more precise physics models, particularly in the areas of current drive and transport. This may entail the inclusion of self-consistent plasma-profile evolution in the modeling analysis. Acquiring ample operational experience in plasma initiation, current start-up, and current ramp-up on a large tokamak reactor, such as ITER, is most important. Similar experience with the auxiliary-heating and density-rise phase, smooth transition from lower-hybrid to fast-wave current drive, and the approach to steady-state burn will be valuable.

The engineering aspect of the reactor plant start-up and operation is also examined in the context of the operational constraints imposed by the major subsystems (first wall, blanket, divertor, and power conversion system) and material choices. It is found that, as long as the superconducting magnets are not de-energized during routine shutdowns, it is the start-up time for the power conversion system that determines the start-up time of the ARIES-I plant. The total start-up time then ranges from twelve hours for cold start-up to two hours for hot start-up, and the orderly shutdown time is approximately two hours. The choice of SiC composite as the first-wall structural material and Li_2ZrO_3 as the breeder material permits, in principle, blanket operation ranging from 10% to 190% of full power. No major critical issue has been uncovered during the course of this investigation.

REFERENCES

- [1] F. C. Jobs, S. Bernabei, T. K. Chu, *et al.*, "Start-Up and Ramp-Up of the PLT Tokamak by Lower Hybrid Waves," *Phys. Rev. Lett.* **55** (1985) 1295.
- [2] S. Itoh, N. Hiraki, Y. Nakamura, *et al.*, "Experiments on Steady-State Tokamak Discharge by LHCD in TRIAM-1M," in *Proc. 13th Int. Conf. on Plasma Phys. and Controlled Nucl. Fusion Research*, Washington, D.C. (Oct. 1990), International Atomic Energy Agency, Vienna (1991).
- [3] T. Imai, "Lower Hybrid Current Drive and Higher Harmonic ICRF Heating Experiments on JT-60," in *Proc. 13th Int. Conf. on Plasma Phys. and Controlled Nucl. Fusion Research*, Washington, D.C. (Oct. 1990), International Atomic Energy Agency, Vienna (1991).
- [4] R. W. Conn, N. M. Ghoniem, and M. A. Firestone, Eds., "Tokamak Reactor Operations Study," University of California Los Angeles report UCLA-PPG-1009 (1986).
- [5] G. V. Pereverzev, "Non-Inductive Startup and Current Ramp-Up Scenario Optimization for a Tokamak Reactor," *Proc. 12th Int. Conf. on Plasma Phys. and Controlled Nucl. Fusion Research*, Nice, France (Oct. 1988), International Atomic Energy Agency, Vienna (1989) 739.
- [6] F. Najmabadi, R. W. Conn, R. A. Krakowski, K. R. Schultz, D. Steiner, and the TITAN Research Group, "The TITAN Reversed-Field-Pinch Reactor Study—The Final Report," University of California Los Angeles, General Atomics, Los Alamos National Laboratory, and Rensselaer Polytechnic Institute, University of California Los Angeles report UCLA-PPG-1200 (1990); also, F. Najmabadi, R. W. Conn, R. A. Krakowski, K. R. Schultz, D. Steiner, and the TITAN Research Group, "Engineering and Physics of High-Power-Density, Compact, Reversed-Field-Pinch Fusion Reactors: The TITAN Study," *Proc. 15th Symp. Fusion Technol. (SOFT)*, Utrecht, the Netherlands (Sept. 1988), *Fusion Technology* **88**, A. M. Van Ingen, A. Nijsen-Vis, H. T. Klippel, Eds., North-Holland, Amsterdam (1989) p. 1779.
- [7] R. L. Hagenon, R. A. Krakowski, C. G. Bathke, *et al.*, "Compact Reversed-Field Pinch Reactors (CRFPR): Preliminary Engineering Considerations," Los Alamos National Laboratory report LA-10200-MS (1984).
- [8] D. A. Ehst, K. Evans, Jr., and W. M. Stacey, "The Influence of Physics Parameters on Tokamak Reactor Design," *Nucl. Technol.* **43** (1979) 28.

- [9] Y. N. Dnestrovski and D. P. Kostomarov, *Numerical Simulation of Plasmas*, Springer-Verlag, Berlin (1985) p. 188.
- [10] M. Y. Hsiao, D. A. Ehst, and K. Evans, Jr., "Bootstrap Currents in Radio-Frequency Driven Tokamak Equilibria," *Nucl. Fusion* **29** (1989) 49.
- [11] R. W. Harvey, "Bootstrap Current," in Ignition Physics Study Group report on Current Drive, Princeton Plasma Physics Laboratory unpublished data (1988).
- [12] R. J. Goldston, "Energy Confinement Scaling in Tokamaks: Some Implications of Recent Experiments with Ohmic and Strong Auxiliary Heating," *Plasma Phys. Controlled Fusion* **26** (1984) 87.
- [13] D. E. Post *et al.*, "Radiative Cooling of Low-Density, High-Temperature Plasma," *Atomic Data and Nucl. Data Tables* **20** (1977) 398.
- [14] T. Okazaki, M. Sugihara, and N. Fujisawa, "Low Hybrid Current Drive in the Presence of a DC Electric Field," *Nucl. Fusion* **26** (1986) 1029.
- [15] Y-K. M. Peng, Fusion Engineering Design Center, Oak Ridge National Laboratory, private communication (1989).
- [16] K. A. Werley, G. L. Varsamis, R. L. Miller, *et al.*, "Burning DT Plasmas in the Reversed-Field Pinch (RFP)," Los Alamos National Laboratory report (in preparation, 1990).
- [17] N. A. Uckan, "ITER Physics Design Guidelines," International Tokamak Experimental Reactor report ITER-TN-PH-8-6 (1988).
- [18] F. Openshaw, General Atomics, private communication (Aug. 1989).
- [19] "Assessments of an Advanced Pulverized-Coal Power Plant," Westinghouse Electric Co., Electric Power Research Institute report EPRI CS-2223 (1982).
- [20] "Assessments of an Advanced Pulverized-Coal Power Plant," General Electric Co and Stone and Webster Engineering Corp., Electric Power Research Institute report EPRI CS-2555 (1982).